# HEADLAND MODELING APPLIED TO THE EASTERN BEAUFORT SEA COAST

by

Thomas L. Kozo, Ph.D.

VANTUNA Research Group

Occidental College

Final Report
Outer Continental Shelf Environmental Assessment Program
Research Unit 519

1984

# TABLE OF CONTENTS

LIST OF FIGURES

# LIST OF TABLES

## ABSTRACT

The United States Coast Guard deployed a cluster of satellite-transmitting, surface-drifting buoys in the Beaufort Sea north of Prudhoe Bay, Alaska on 17 August 1983. The surface currents in this coastal area are predominantly wind driven. An unusual stand of westerly winds led to eastward drift with the surviving buoys moving into an area north of Mackenzie Bay (Canada) by mid-October. The buoy motion suggested that they were driven by the geostrophic wind modified by the orographic "umbrella" of the Brooks Range. The mountain influence was seen to cover an arcuate zone at least 100 km seaward of the coast from Camden Bay (Alaska) to Mackenzie Bay. This is a headland effect on the wind of major proportions creating changes in direction and regions of super and subgeostrophic speeds over the coastal zone.

A simple model was developed to predict the wind modifications in this headland zone and the resultant wind-driven buoy drift. The initial wind velocity input to this model is a calculated geostrophic wind derived from triangular-shaped mesoscale atmospheric pressure networks. These networks were chosen because their boundaries alternately contained the trajectories of the eastward-moving buoys. The model then used this network velocity to generate the wind field at the buoy location and appropriate offshore area north of the Brooks Range. The mountain barrier was taken to have approximate cylindrical geometry and atmospheric flow conditions were assumed to be irrotational and non-divergent.

The actual buoy drift during the open water season covered 650 km in 60 clays with the final model-predicted buoy-drift position in error by less than

50 km. The major error occurred when the buoys moved into shallow water in the Mackenzie Bay on 21 September 1983. One buoy was destroyed and the other was constrained to move parallel to the 10 m bottom contour. The Brooks Range influence did not appear to affect the October buoy drift which was north of Richards Island (Canada) above 70°N and east of 135°W.

# INTRODUCTION

A headland or promontory (Crossley, 1938) of sufficient height and lateral dimensions will modify the large scale wind and pressure fields. Flow around an obstacle requires less energy than flow over the same obstacle in a stable atmospheric boundary layer, which often exists in arctic regions in all seasons (Kozo, 1984a, 1982). Zones of accelerated and decelerated, diverted flow will reach offshore from headlands for distances equal to the lateral dimensions of the obstacle (usually mesoscale effects). The exact positions of these stagnation or acceleration zones will shift with the direction of the incoming large-scale wind. Since ocean surface pollutant residence times the trajectories are of major concern in coastal zones, a model predicting the lateral extent and location of "abnormal" winds can be very useful. The utility is magnified in coastal *zones* such *as* found *in* the Alaskan Beaufort where the surface currents are primarily wind driven (Aagaard, 1984).

A simple model utilizing combinations of mesoscale atmospheric pressure networks (Kozo, 1980, 1982, 1984a) to calculate high resolution calculated geostrophic winds for initial input has been developed. This model then computes a new wind velocity for designated offshore areas as modified by flow around the Brooks Range. The method was pioneered by Dickey (1961) but extends his concepts spatially from land to offshore and temporally from winter to summer. Dickey (1961) approximated the 600 m contour of the Brooks Range (see Fig. 1) as a cylindrical barrier and calculated the velocity field around this barrier using basic hydrodynamical equations (i.e., Batchelor, 1967). His analysis was then used to explain the supergeostrophic

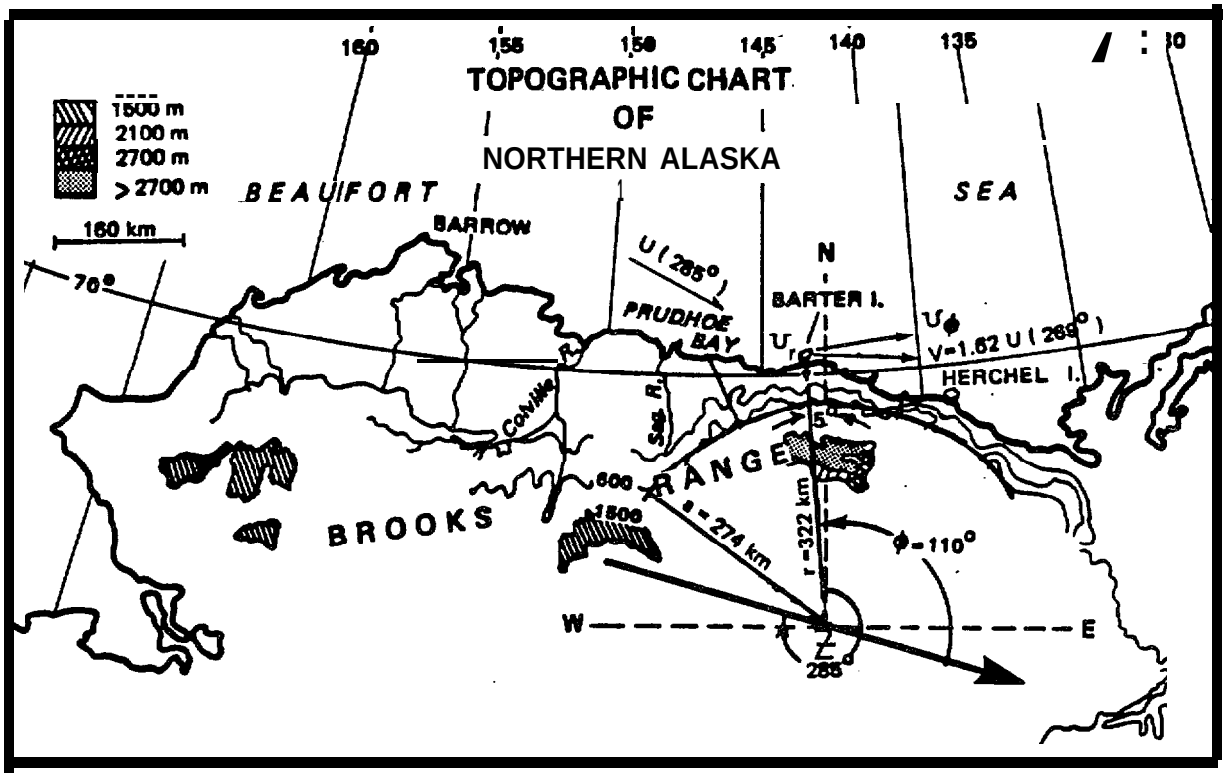


Figure 1. Topographic chart of northern Alaska (after Dickey, 1961) showing the 600 m contour of the Brooks Range approximated as a circular arc. Its radius (a) is computed to be 274 km and its hypothetical center is Z. The distance from Z to Barter Island is 322 km.

winds at Barter Island (Fig. 1), a main observation point on the Alaskan Beaufort coast. Twenty-four years later NOAA/MMS field work has expanded the data base offshore (Kozo, 1980, 1984a). In addition, the United States Coast Guard (Robe *et al.* 1984) has recently obtained buoy drift data (position and time) which have shown open-water movement characteristics that could only be explained by Dickey's (1961) original hypothesis. Therefore, matching the empirical buoy drift positions with model buoy drift positions has provided a means of predicting wind modification zones and buoy movement as well.

## STUDY AREA

Figure 1 shows the Beaufort Sea coast of Alaska and Canada with the 600 m contour of the Brooks Range approximated as a cylinder with a 274 km radius (z-axis vertical). Moving eastward, this contour approaches to within 40 km of the coast and stays even closer until well past Herschel Island (Canada). The coastal zones offshore from this encroaching mountain range will be subject to stable boundary layer induced orographic effects in winter or summer (Kozo, 1984a; see summer temperature profiles) which can dominate winds at least 100 km seaward (Kozo 1984b). Orographic effects several 100 km offshore have been documented in the Antarctic (Schwerdtfeger, 1979).

The mid-shelf (~ 50 m isobath) surface currents along the Alaskan Beaufort Sea coast are mainly wind driven (Aagaard, 1984). The typical wind direction at most surface data stations (Brewer *et al.*, 1977) is from the northeast resulting in a net westward drift. Sea ice dominates this same coastal zone, covering it for at least nine months each year (open water season, about mid-July to mid-October). Again, it is the winds that play a major role in the sea ice edge position in these open water months (Kozo, 1984a). Results of Arctic research since the 1970's have shown that large

scale (synoptic-scale) weather map analyses have been inadequate for predicting surface winds or ice edge motion in the Alaskan Beaufort coast region (Rogers, 1978; Albright, 1978; Kozo, 1980). The main reason was the lack of National Weather Service (NWS) stations with only Barrow and Barter Island (Fig. 1) covering 540 km of coastline. There were none north of the coast, on a continuous basis, until the Arctic Basin Buoy Project (National Science Foundation) *was* begun in February 1979. The other reasons are the arctic sea breeze (Kozo, 1982) and the orographic modifications on the large scale **wind produced by the Brooks Range for at least 50% of the Alaskan Beaufort coast. For the purposes of this study the sea breeze effect has been shown to be minimal 20 km seaward of the coast (Kozo 1982) and cannot be evaluated by examination of the Coast Guard buoy tracks,**

## DATA

### PRESSURE DATA

Barometric pressure data reduced to sea level and temperature data were taken simultaneously from three-station weather networks and used to compute hypothetical geostrophic winds for the area enclosed by each network (Fig. 2). The stations A (Barrow), C (Barter Island), D (Inuvik, Canada) and E (Tuktoyaktuk, Canada) are part of a global weather network (first order stations) and transmit real-time data to the National Meteorological Center (NMC). The accuracies of their pressure and temperature data are better than ± .25 mb and ± 1°C respectively. Station B (Franklin Bluffs) was an unmanned satellite-transmitting pressure, temperature and position platform operating through System ARGOS and manufactured by Polar Research Laboratory in Santa Barbara, California. ARGOS is a cooperative project between Center National d' Etudes Spatiales (NES, France), National Aeronautics and Space

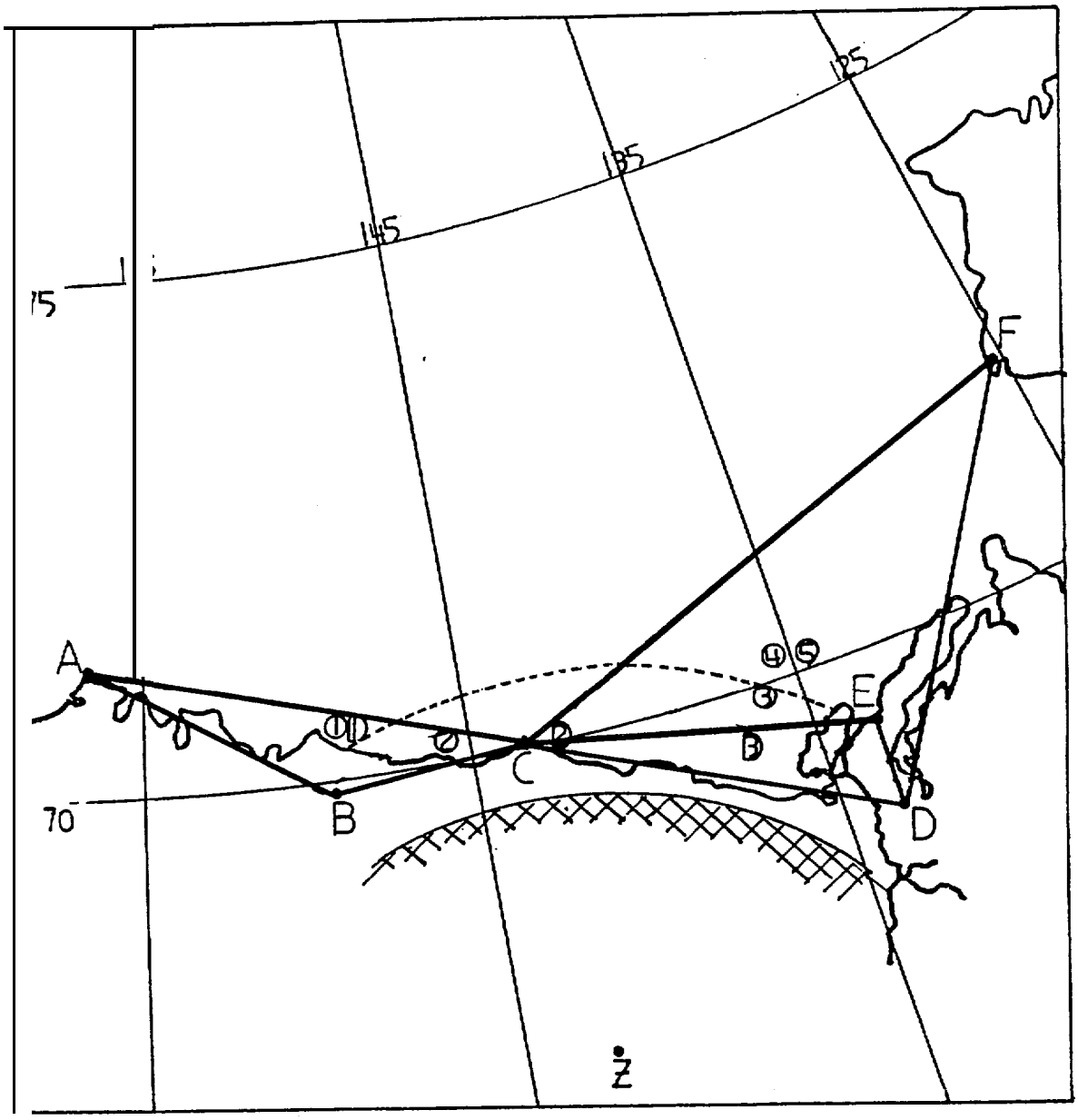


Figure 2. pressure triangles used to compute geostrophic winds for August (ABC), September (CDE), and October (CFD) 1983. Data stations are Barrow (A), Franklin Bluffs (B), Barter Island (C), Inuvik (D), Tuktoyaktuk (E) and Sachs Harbor (F). O ≡Buoy 4519. D ≡ 4518 (died 24 September 1983, position #3). Buoy position numbers 1-2 (August), 2-4 (September), 4-5 (October) indicate positions relative to pressure triangles. The dashed arc is the probable distance seaward of major orographic influence from the 600 m contour (cross hatched). Z ≡ hypothetical center of the circle matching the arc.

Administration (NASA, U.S.) and the National Oceanic and Atmospheric Administration NOAA, U.S.). The pressure and temperature data accuracies were also better than ± .25 mb and ± 1°C respectively since both were comparison calibrated to the Barrow and Barter Island station instruments. Station F (Sachs Harbor) is an airport weather station that reports four times a day (six-hourly). No check has been made on its data accuracy. The eastward buoy trajectories made it a necessary network input, however.

## GEOSTROPHIC WIND DATA

These data were computed from the pressure and temperature data triangles shown in Figure 2. Three triangles were chosen from five (original ones) because they fit certain criteria: buoy trajectory coverage, output compatibility with buoy motion, and availability of data.

The atmospheric flow was assumed to be in geostrophic balance (l):

$$f(\underset{\sim}{k} \times \underset{\sim}{V}_G) + \frac{\nabla P}{\rho} = 0 \qquad (1)$$

The first term is the Coriolis force, and the second is the pressure gradient force with f the Coriolis parameter ($1.37 \times 10^{-4}$ $sec^{-1}$ at 70° N), k the vertical unit vector, $V_G$ the geostrophic velocity vector, $\nabla P$ the gradient of the atmospheric pressure, and $\rho$ the air density. Using the station combination of triangle ABC (Fig. 2) for example, and noting that pressure can be represented as a function of latitude (y) and longitude (x) on a plane surface:

$$\begin{aligned} P_A(x,y) &= ax_A + by_A + c \\ P_B(x,y) &= ax_B + by_B + c \\ P_C(x,y) &= ax_C + by_C + c \end{aligned} \qquad (2)$$

Here the subscripts A, B, C denote their respective stations. Cramer's rule

or a least squares fitting technique (Kozo, 1982) can be applied to (2) to solve for unknowns a, b, c. Since $\frac{dP}{dx} = a$ and $\frac{dP}{dy} = b$, the pressure gradient VP can be determined. Use of (1) results in $V_G$ since f is known and p for dry air can be determined from station temperatures.

Station errors of ± 1°C can cause errors of .34% in the velocity magnitude since they effect p estimates. Calculated geostrophic winds less than 2 $ms^{-1}$ are suspect since pressure errors (see above) can create maximum speed errors (Kozo, 1982) greater than ± 1.35 ins-l and direction errors greater than ± 40° for triangle ABC. The error will be approximately the same for triangle CED and less for large triangle CFD if station F is reliable (see Fig. 2).

Bivariate distributions of calculated geostrophic wind speeds versus wind directions are shown for the months of August (Table 1, ΔABC), September (Table 2, ΔCDE) and October (Table 3, ΔCDF). It can be seen that the dominant wind directions were from the NW-W in August, September, and October, which accounted for the observed eastward buoy drift.

## BUOY POSITION DATA

The data buoys deployed in open water on August 1983 by the U. S. Coast Guard were tracked by NOAA polar orbiting satellites through use of a position transponder called an ARGOS Data Acquisition Platform (ADAP), Model 901. Each ADAP platform position is received 8-12 times per day with an accuracy of approximately 300 m (Bessis, 1981). The buoy hulls have a ratio of submerged area to exposed area of at least 2:1. Therefore wind stress on the hull itself does not dominate buoy motion. The best assumption is that the buoys follow the wind-driven currents in the upper 1-2 m of the water column.

Table 1. Calculated geostrophic wind speed ($ms^{-1}$) vs. direction for August 1983.

| WIND DIR. | WIND VEL. (M/S) 0- 2 | 2- 4 | 4-6 | 6-6 | 8-10 | 10-12 | 12-14 | 14-16 | 16-18 | 16-28 | 2?-222?-24 | 24-25 | 25-28 | 28-30 | TOTA. | PER |
|---|---|---|---|---|---|---|---|---|---|---|---|---|---|---|---|---|
| 326. *348.5 | 1 | 2 | 0 | 1 | 0 | 0 | 0 | 0 | 0 | e | 0 | e | e | 0 | 0 | 4 | 1.8 |
| 383.5-326.9 | 3 | 4 | 0 | 1 | 1 | 0 | 0 | e | 0 | 0 | e | e | 0 | 0 | e | 9 | 3.0 |
| 261.0-303.5 | 4 | 3 | 7 | 3 | 6 | 7 | 1 | 0 | 0 | e | a | 0 | 0 | 0 | [illegible] | 31 | 12. 0 |
| 258.5-281.0 | 2 | 7 | 11 | 5 | 15 | 3 | e | e | e | e | 0 | e | 0 | 0 | e | 43 | 17. 0 |
| 236.0-258.5 | 0 | 5 | 2 | 4 | 4 | 9 | 3 | 2 | 1 | 1 | 0 | 0 | e | 0 | e | 31 | 12. 0 |
| 213.5-236.0 | 1 | 3 | 2 | 1 | 1 | 5 | 1 | e | e | 0 | 0 | e | e | 0 | 0 | 14 | 5. e |
| 191.0-213.5 | 1 | 4 | 4 | 3 | 0 | 0 | 0 | e | e | 0 | 0 | 0 | e | 0 | 0 | 12 | 4. 0 |
| 168.5-191.0 | 0 | 1 | a | 1 | 1 | e | e | e | 0 | 0 | e | 0 | e | 0 | e | 11 | 4. B |
| 146.0-168.5 | 1 | 3 | 5 | 4 | 1 | 1 | 0 | e | e | 0 | e | 0 | 0 | 0 | 0 | 15 | 6.0 |
| 123.5-146.0 | e | 0 | 2 | 0 | 3 | 1 | 1 | 1 | e | 2 | e | 0 | e | 0 | 0 | 10 | 4.@ |
| 101. 0-123.5 | 0 | 1 | 4 | 4 | 5 | 9 | 2 | 1 | [illegible] | 1 | e | 0 | 0 | 0 | 0 | 26 | 11.0 |
| 78.5-101.0 | 2 | 2 | 0 | 3 | 0 | 0 | 2 | 3 | 1 | 0 | 1 | e | e | 0 | e | 14 | 5.0 |
| 56.0- 76.5 | 1 | 2 | [illegible] | 8 | 1 | 2 | 0 | 0 | 0 | 0 | 0 | 0 | e | 0 | e | 7 | 2.0 |
| 33.5- 56.0 | 0 | 3 | 0 | 1 | e | 0 | e | e | e | 0 | 0 | 0 | e | 0 | 0 | 4 | 1.0 |
| 11.0- 33.5 | 4 | 3 | 4 | 1 | e | 0 | e | 0 | e | 0 | 0 | 0 | 0 | 0 | e | 12 | 4.% |
| 346. s- 11.0 | 0 | 1 | 1 | 1 | e | e | e | e | 0 | e | e | e | 0 | 0 | e | 3 | 1.0 |

Table 2. Calculated geostrophic wind speed (ms$^{-1}$) vs. direction for September 1983.

| WIND DIR. | WIND VEL. (M/S) 8-2 | 2-4 | 4-6 | 6-8 | 8-10 | 10-12 | 12-14 | 14-16 | 16-18 | 18-20 | 20-22 | 22-24 | 24-26 | 26-28 | 28-30 | TOTAL | PER |
|---|---|---|---|---|---|---|---|---|---|---|---|---|---|---|---|---|---|
| 326.2-346.5 | 1 | 4 | 3 | 4 | 7 | 2 | 1 | 0 | 0 | 0 | 0 | 0 | 0 | 0 | 0 | 22 | 9.0 |
| 383.5-326.0 | 1 | 3 | 3 | 3 | 2 | 0 | 1 | 0 | 2 | 0 | 0 | 0 | 0 | 0 | 0 | 15 | 6.0 |
| 281.2-3$3.5 | 3 | 5 | 5 | 0 | 0 | 0 | 0 | 0 | 0 | 0 | 0 | 0 | 0 | 0 | 0 | 13 | 5.0 |
| 2s2.s-221.0 | 3 | 3 | 6 | 4 | 0 | 0 | 0 | 0 | 0 | 8 | 0 | 0 | 0 | 0 | 0 | 16 | 6.0 |
| 236.2-252.5 | 2 | 2 | 3 | 5 | 1 | 0 | 0 | 0 | 0 | e | 0 | 0 | 0 | 0 | 0 | 13 | 5.0 |
| 213.S-236.0 | 2 | 2 | 2 | 2 | 2 | 0 | 0 | 0 | 0 | 0 | 0 | 0 | 0 | 0 | 0 | 18 | 4.0 |
| 191.0-213.5 | 3 | 5 | 7 | 4 | 2 | 1 | 1 | 0 | 0 | 0 | 0 | 0 | 0 | 0 | 0 | 23 | 9.0 |
| 168.5-191.0 | 1 | 4 | 9 | 4 | 1 | 0 | 0 | 0 | 0 | 0 | 1 | 0 | 0 | 0 | 0 | 26 | 10.0 |
| 146.2-162.5 | 3 | 5 | 2 | 3 | 2 | 3 | 2 | 1 | 1 | 1 | 2 | 0 | 0 | 0 | 0 | 25 | 10.0 |
| 123.5-146.0 | 2 | 0 | 4 | 1 | 2 | 1 | 0 | 0 | 0 | 0 | 0 | 0 | 0 | 0 | 0 | 10 | 4.0 |
| 101.0-123.5 | 3 | 4 | 1 | 0 | 0 | 0 | 0 | 0 | 0 | 0 | e | 0 | 0 | 0 | 0 | 8 | 3.0 |
| 780 5-101.0 | 3 | 5 | 1 | 0 | 0 | 0 | 0 | 0 | 0 | 0 | 0 | 0 | 0 | 0 | 0 | 9 | 3.0 |
| 56.0-78.5 | 3 | 2 | 2 | 0 | 0 | 0 | 0 | 0 | 0 | 0 | 0 | 0 | 0 | 0 | 0 | 7 | 2.0 |
| 33.s- 56.0 | 3 | 2 | 1 | 2 | 0 | 0 | 0 | 0 | 0 | 0 | 0 | 0 | 0 | 0 | 0 | 8 | 3.0 |
| 11.6 -33.5 | 2 | 2 | 1 | 3 | 4 | 1 | 0 | 0 | 0 | 0 | 0 | 0 | 0 | 0 | 0 | 13 | 5.0 |
| 342.s- 11.0 | 3 | 1 | 10 | 3 | 2 | 0 | 1 | 1 | 1 | 0 | 0 | 0 | 0 | 0 | 0 | 22 | 9.0 |

Table 3. Calculated geostrophic wind speed ($ms^{-1}$) vs. direction for October 1983.

| WIND DIR ° | WIND VEL. (M/S) e-2 | 2-4 | 4-6 | 6-8 | 6-10 | 10-12 | 12-M | 14-16 | 16-18 | 18-22 | 20-22 | 22-24 | 24-26 | 26-28 | 26-30 | TOTAL | PER |
|---|---|---|---|---|---|---|---|---|---|---|---|---|---|---|---|---|---|
| 326.0-340.5 | 0 | 2 | 4 | 1 | 2 | 0 | 0 | 0 | e | 0 | 0 | 0 | e | 0 | 0 | 9 | 7.0 |
| 303.5-326.0 | 0 | 3 | 1 | 5 | 3 | 1 | 0 | 0 | 0 | 0 | e | 0 | 0 | e | e | 19 | 1s.0 |
| 281.2-303.5 | 0 | 2 | 1 | 3 | 2 | 2 | 0 | 0 | e | 0 | 0 | e | 0 | 0 | e | 10 | 8.0 |
| 23.s281.0 | 0 | 0 | 1 | 1 | 0 | 0 | 0 | 0 | 0 | 0 | 0 | 0 | e | e | e | 2 | 1.0 |
| 236.0-258.5 | 1 | 2 | 0 | 1 | 0 | 0 | 0 | 0 | e | 0 | 0 | 0 | 8 | 0 | 0 | 4 | 3.8 |
| 213.5-2? 6.0 | 0 | 1 | 0 | 1 | 0 | 1 | 0 | 0 | 0 | 0 | e | 0 | 0 | 0 | 0 | 3 | 2.0 |
| 191.0-213.5 | 3 | 1 | 1 | e | 1 | 0 | 1 | 0 | 0 | 0 | 0 | 0 | 0 | e | 0 | 7 | s.1 |
| 168.5-191.0 | 2 | 2 | 2 | 1 | 0 | 0 | 1 | 0 | e | 0 | 0 | 0 | 0 | 0 | 0 | 8 | 6*8 |
| 146.0-168.5 | 1 | 0 | 0 | 3 | 0 | 1 | 0 | 0 | 0 | 0 | 0 | 0 | 0 | 0 | 0 | 5 | 4.e |
| 123.5-146.0 | 1 | 0 | 1 | 2 | 1 | 1 | 0 | 1 | 0 | 0 | 0 | 'e | e | e | 0 | 7 | 5.0 |
| 101.0-123.5 | 2 | 6 | 3 | 3 | 3 | 0 | 0 | 0 | 0 | 0 | 0 | 0 | e | e | 0 | 17 | 13.0 |
| 72.5-101.0 | 0 | 2 | 2 | 0 | 2 | 1 | 0 | 0 | 1 | 0 | e | 0 | 0 | e | e | 8 | 6.0 |
| 56. 0- 78.5 | 4 | 0 | 1 | 0 | 1 | 0 | 0 | 0 | 1 | 0 | 0 | 0 | 0 | e | 0 | 7 | "5.6 |
| 33.5- 56.0 | 2 | 1 | 3 | 0 | 0 | 0 | 0 | 0 | 1 | 0 | 0 | 0 | 0 | 0 | 0 | 7 | 5.0 |
| 11.0- 33.5 | 1 | 1 | 5 | 1 | 0 | B | 0 | 0 | 0 | 0 | 0 | 0 | 0 | 0 | e | 8 | 6.0 |
| 348.5- 11.0 | 0 | 1 | 2 | 0 | e | 0 | 0 | 0 | 0 | 0 | 0 | 0 | 0 | 0 | e | 3 | 2.0 |

The open-water buoy trajectory chosen to match the model output was a composite of the two longest surviving buoy trajectories for periods free of interference from offshore islands or shoaling areas. The air temperatures near the coast reached -20°C by 18 October 1983 and remained at or below this level for the rest of the month. This coincided with greatly reduced buoy motion for relatively strong wind fields, characteristic of buoy motion for conditions of total ice cover. Therefore, this became the last date for comparison to the open-water, wind-drift model.

# RESULTS WITH DISCUSSION

## MODEL DESCRIPTION-WINDS

The geostrophic wind velocities computed from the appropriate surface pressure networks (discussed above) are used as initial input to the model. The model given this velocity ($V_G$) and a buoy latitude and longitude will compute a new wind velocity (U) based on this position relative to the center (z) of the hypothetical cylinder approximating the 600 m contour of the Brooks Range (Fig. 1). To get this orographically modified wind the expressions for the velocity distribution around a cylinder in steady, horizontal, irrotational frictionless flow of an incompressible fluid are [Dickey, 1961; see Fig. 1):

Radial velocity component $$U_r = V_G(1-a^2/r^2)\cos\Phi \quad (3)$$

Directional velocity component $$U_\Phi = -V_G(1+a^2/r^2)\sin\Phi \quad (4)$$

Magnitude $$u = (U_r^2 + U_\Phi^2)^{\frac{1}{2}} \quad (5)$$

where a is the radius of the cylinder (274 km), r is the distance to a measuring station or buoy from z and $\Phi$ is the angle from the head of $V_G$ to r. For example, to obtain the probable effects at Barter Island upon a westerly $V_G$ from 285°: let a = 274 km, r = 322 km and $\Phi$ = 110°. From (3-5), $U_r$ = -.095 $V_G$ $U_\Phi$ = -1.619$V_G$ and the modified wind vector U = 1.62$V_G$ from 269°.

The input velocity used in this model differs from that of Dickey (1961). He did not use $V_G$ in (3-5), but a surface wind ($V_S$) taken as .9$V_G$ with a cross isobaric angle (et) of 25°. Taking Barter Island as his main observation point, he matched derived synoptic wind fields from data-limited NWS charts to measured surface winds at land stations. In relatively flat

areas free from orographic influences on the Arctic pack ice, Albright (1980) showed $V_S$ to be .585 $V_G$ with $\alpha$ = 25.9°. Dickey's (1961) main data site was contaminated by interaction with orography and should not have been used. It was surprising that his cross isobaric angle was so close to the more recent work, but the surface speed was obviously affected. This investigator recognizes that adequate information regarding the stability of the boundary layer over the Arctic Ocean is rare and that the primary area of the study will be contaminated by orographic influence. Also, counterclockwise geostrophic departure of the wind due to surface friction in the atmospheric Ekman layer is usually counteracted by clockwise departure from the applied wind stress direction in the oceanic Ekman layers. Therefore, $V_G$ is used directly with no speed reduction or cross isobaric angle applied prior to insertion in (3-5). U is considered the approximate orographically-modified surface wind.

This assumption was tested on some more recent land data shown in Figure 3 (Henry, 1975). Sites L (Lonely) and O (Oliktok) show surface winds from the northeast to east while C (Barter Island), I (Inuvik) and T (Tuktoyaktuk) show surface winds from the northwest. This is obvious evidence for some type of redirected flow around an approximately cylindrical object. $V_G$ can be estimated from the isobaric spacing (Fig. 3) as 17.9 $ms^{-1}$ from 340°. Remembering Figures 1 and 2, r = 480 km, $\Phi$ = 195° and r = 322 km, $\Phi$ = 165° for sites O and C, respectively. Since a = 274 km for both sites, application of (3-5) results in U = .52$V_G$ from 296° for C and u = .73$V_G$ from 27.2° for O. The surface wind flags at C and O show (Fig. 3) a speed of .55$V_G$ from 315° and a speed of .42$V_G$ from 40°, respectively. The directional fit is close with only the speed at O exhibiting large error. This result is very encouraging since the change in direction along the

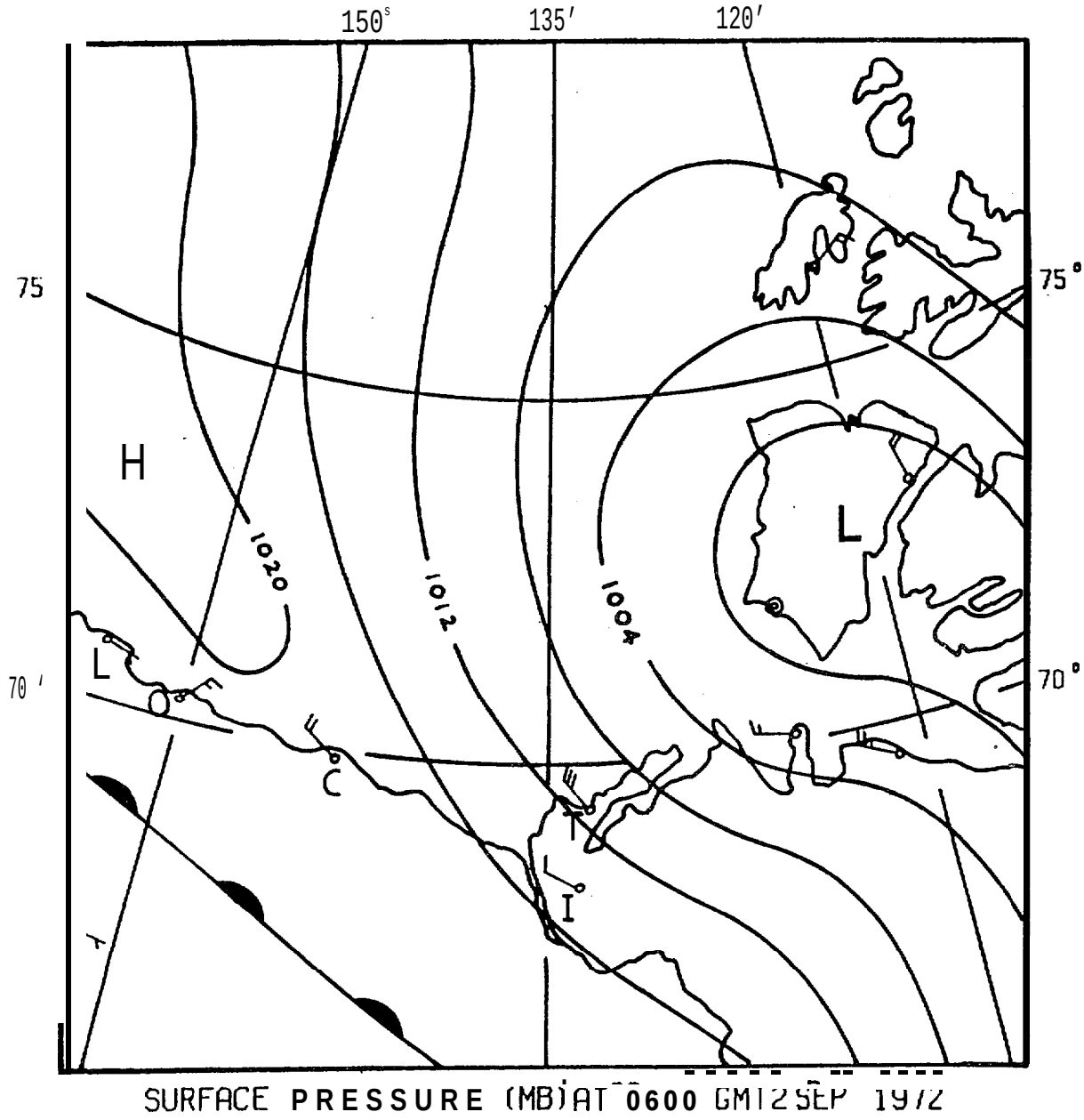


Figure 3. Surface pressure weather map (from Henry, 1975) showing resulting surface winds at shore stations. (Short flags ~ 1.5-3.5 $ms^{-1}$; long flags ~ 4.0-6.0 $ms^{-1}$).

coastline is explained and the speeds are of the correct magnitudes despite the gross approximation of $V_G$ from the weather map.

Figure 4 (Dickey, 1961) displays the streamlines and the velocity field around a cylindrical barrier for conditions of irrotational, non-divergent flow of an undisturbed velocity ($V_\infty$ in the case of this model) from 285°. The numbers at points along the streamlines (showing direction) are wind speeds in multiples of $V_G$. Zones A and B are areas of subgeostrophic and supergeostrophic speeds, respectively. The major influence on the winds" is seen to extend approximately one radius (theoretically) away from the hypothetical cylinder. The A zones cover 30° of arc and the B zones cover 60° of arc. The 600 m elevation does not represent a complete cylinder (see Fig. 1), therefore, $V_G$'s from 120° to 270° are not operated on by the model since they would be coming from behind the mountain range. However, th-ese $V_G$'s are obtained from triangular networks which indicate the mesoscale pressure field north of the Brooks Range so they are preserved at the original calculated velocities. Use of a NWS synoptic surface chart to "guess" at the surface wind for headings from 120° to 270° would also be unwise due to blockage effects on winds from behind the mountains (Kozo, 1984c).

Figures 5-9 show model generated U velocities in multiples of $V_G$ magnitudes as they apply to the Alaska Arctic in a theoretical coastal zone 200 km wide for $V_G$'s from the west, northwest, north, northeast and east, respectively. It should be remembered that a different wind is "created" at each buoy location or study site for a given $V_G$. Examination of Figures 1 and 2 shows that if a given $V_G$ direction is greater than 180°+ (direction from site to Z), the site will be subject to counterclockwise (CCW) flow around the mountain barrier or a westward push. Also, if a given $V_G$ direction is

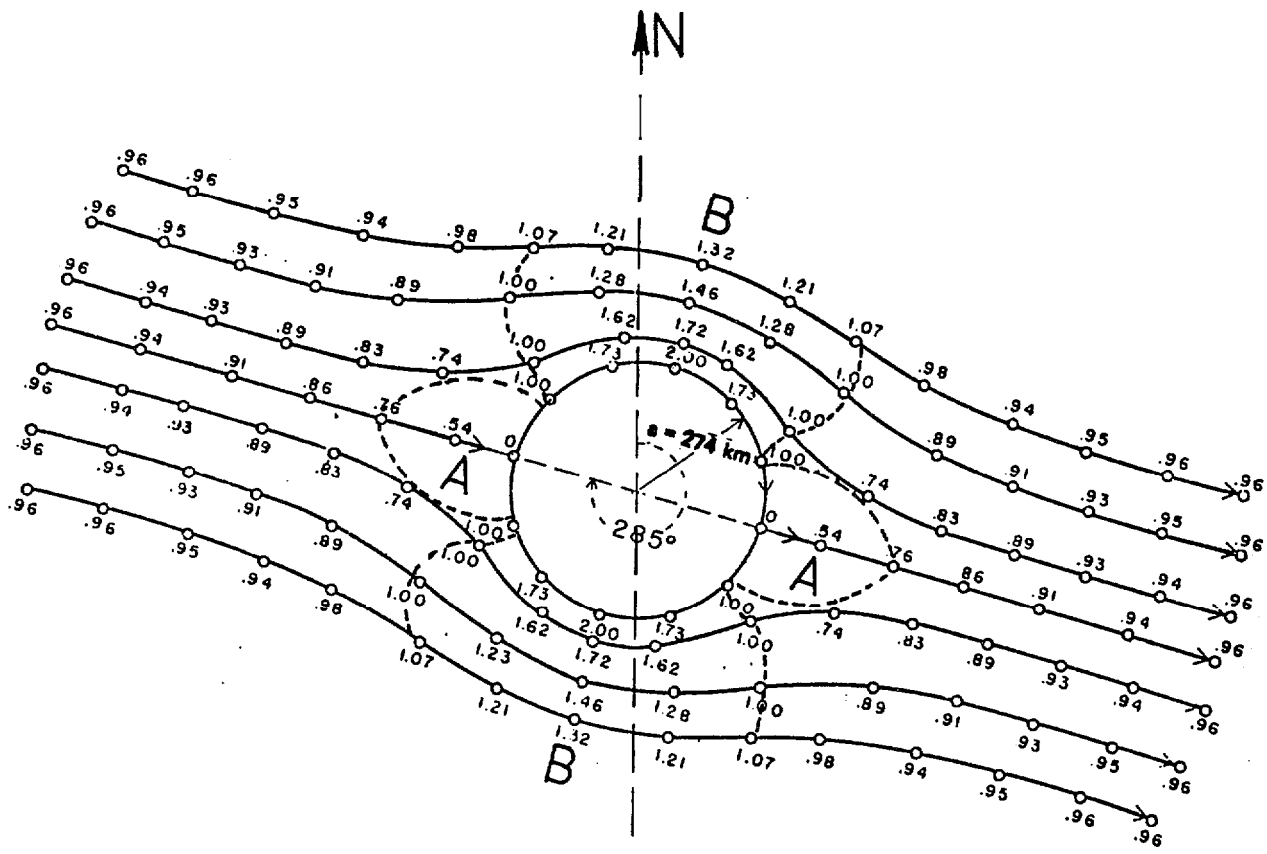


Figure 4. **Streamlines and velocity field around a fixed cylindrical barrier (Dickey, 1961) for irrotational, non-divergent flow of $V_G$. Numbers at points along the streamlines are wind speeds in multiples of the "$V_G$". The B zones indicate higher than normal speeds and the A zones indicate reduced speeds.**

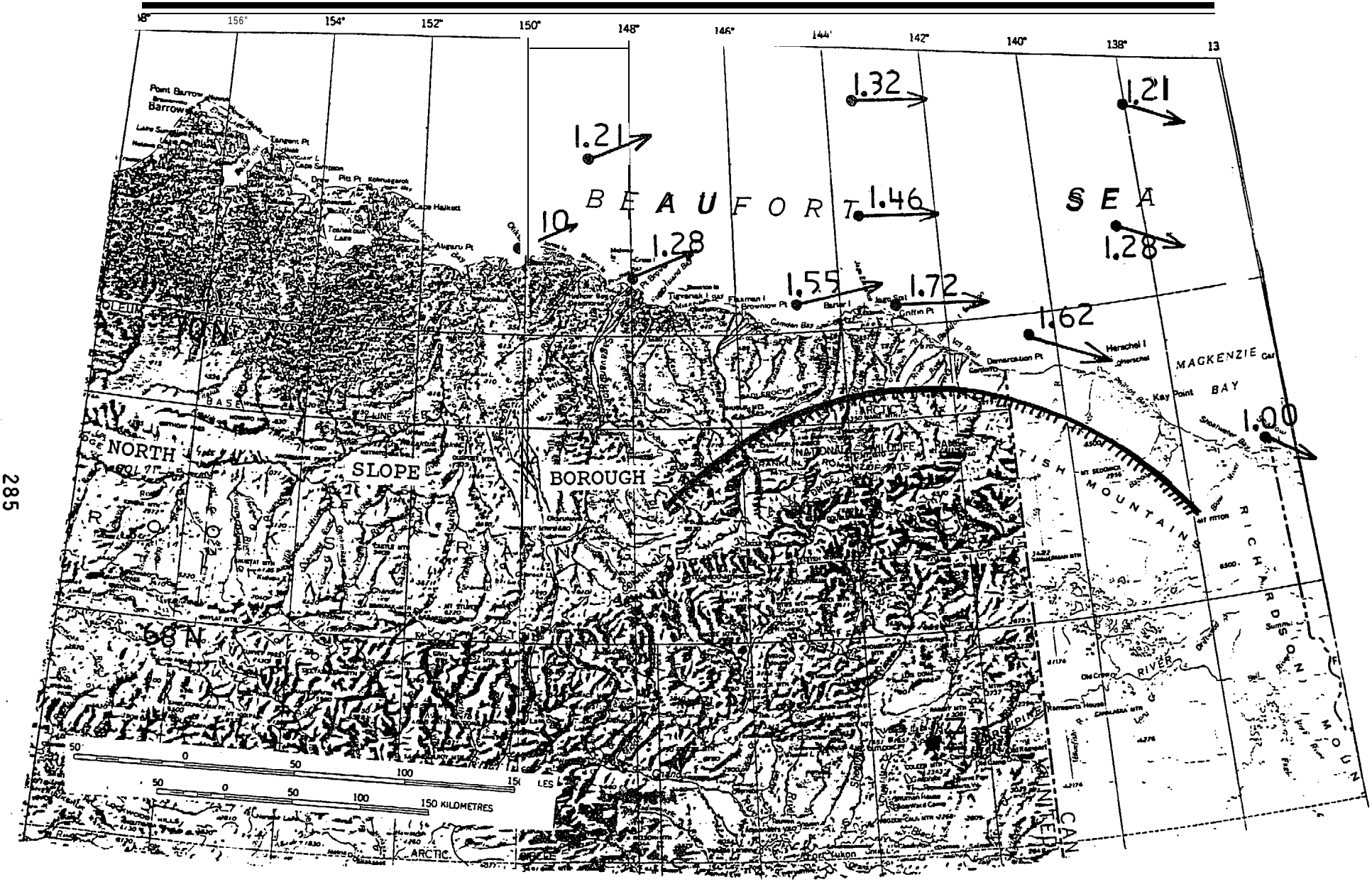


Figure 5. Model generated U velocities in multiples of $V_G$ magnitudes for $V_G$'s from the west.

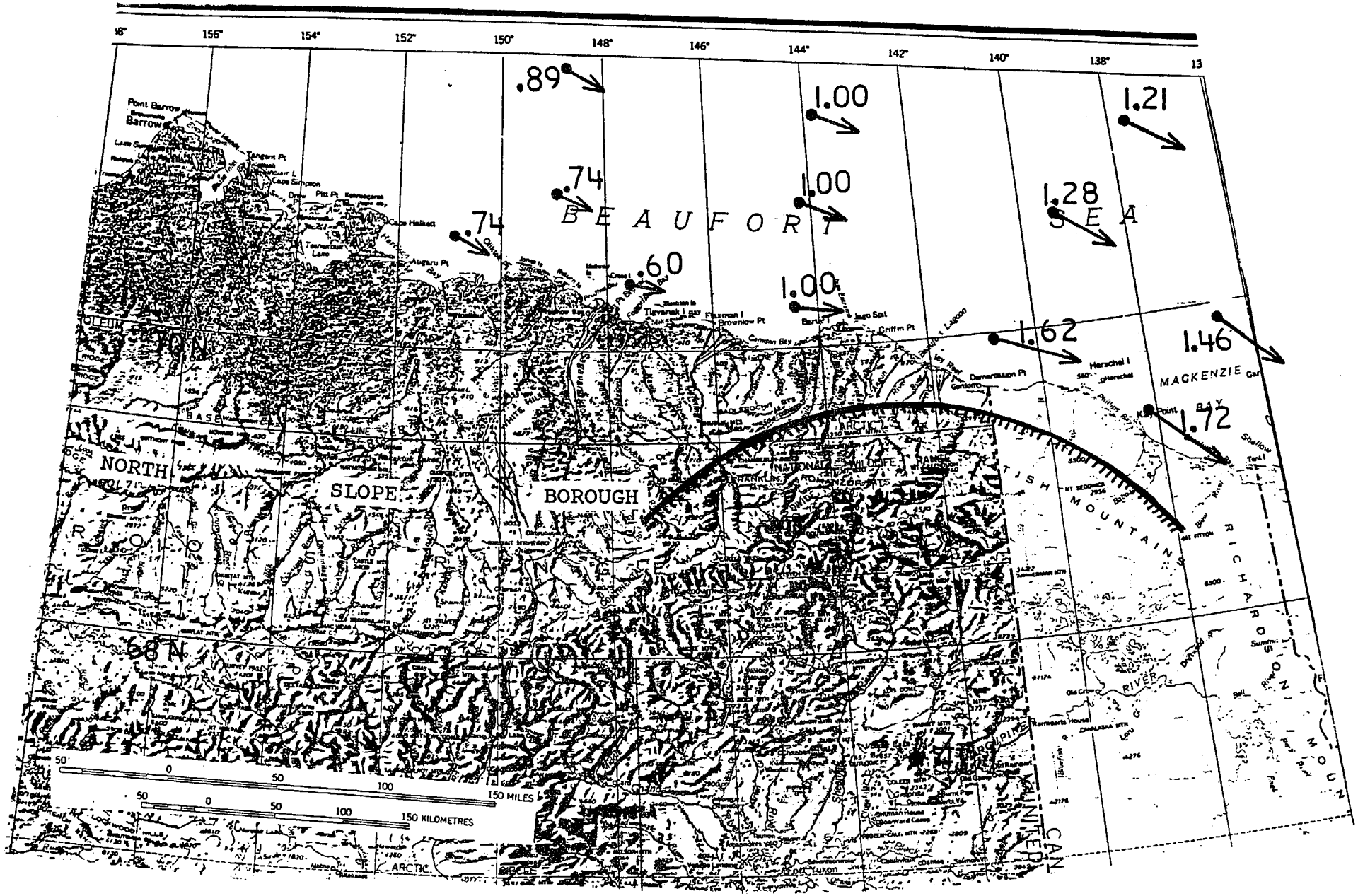


Figure 6. Model generated U velocities in multiples of $V_G$ magnitudes for $V_G$'s from the northwest.

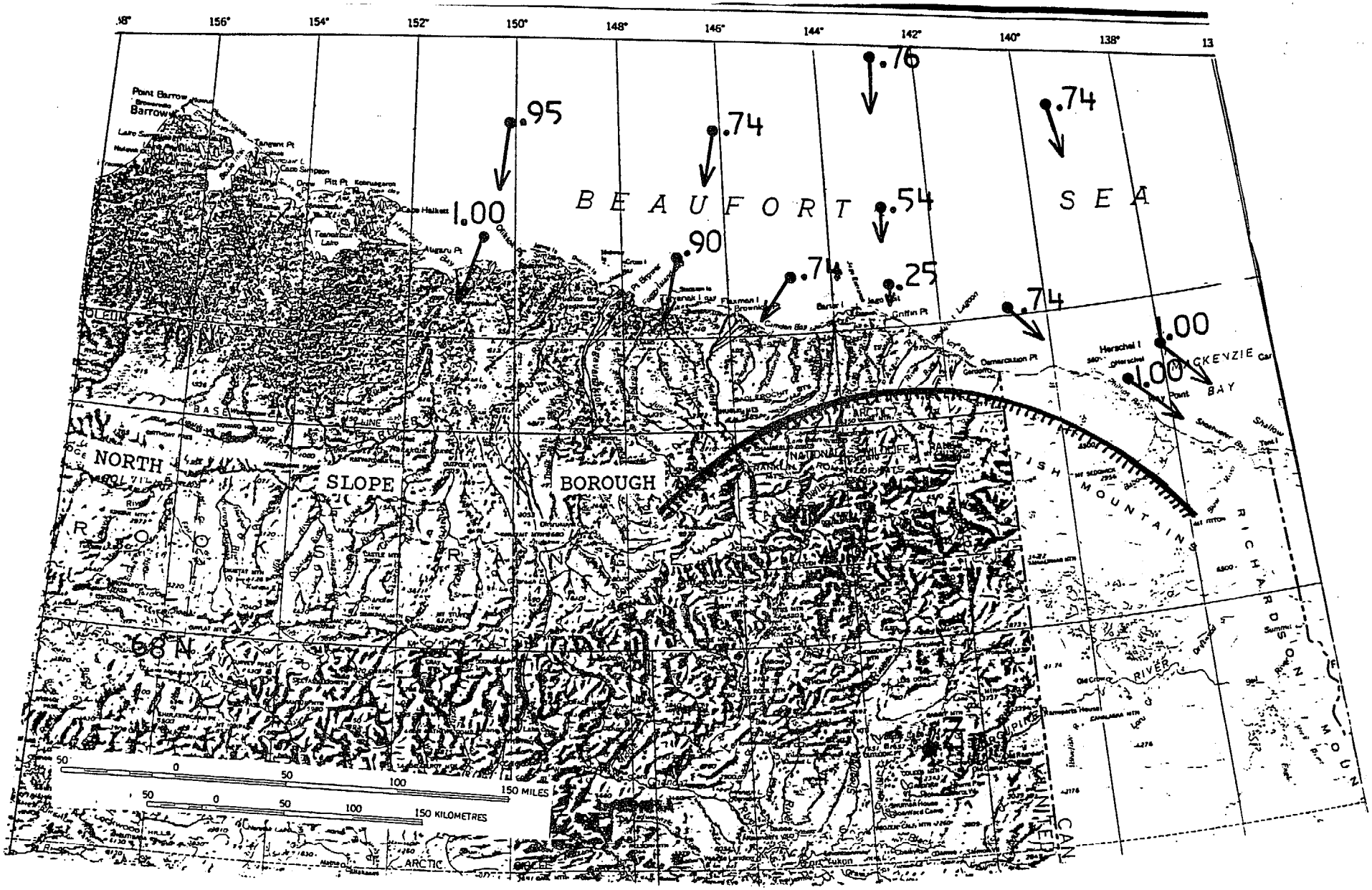


Figure 7. Model generated U velocities in multiples of $V_G$ magnitudes for $V_G$'s from the north.

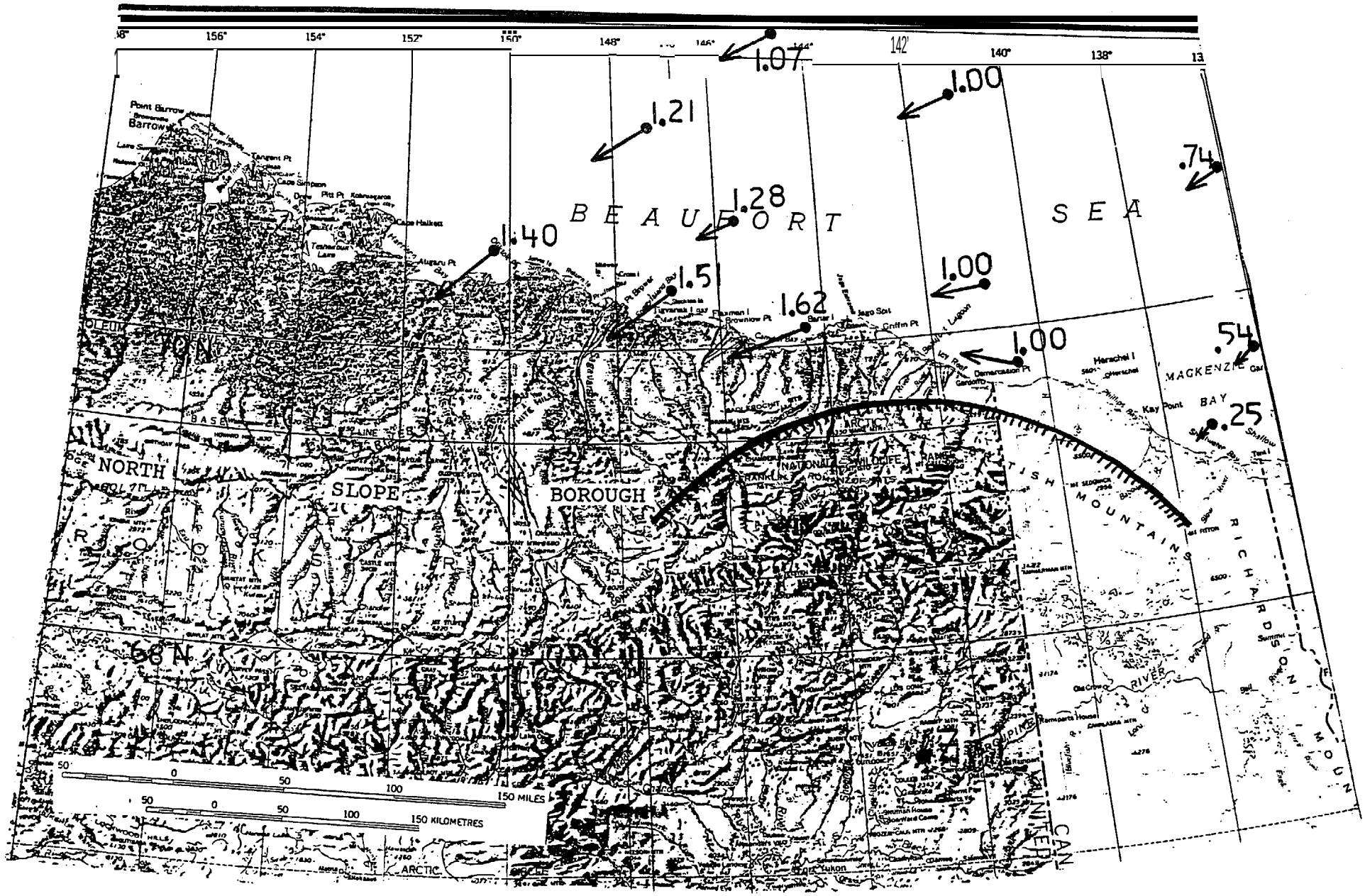


Figure 8. Model generated U velocities in multiples of $V_G$ magnitudes for $V_G$'s from the northeast.

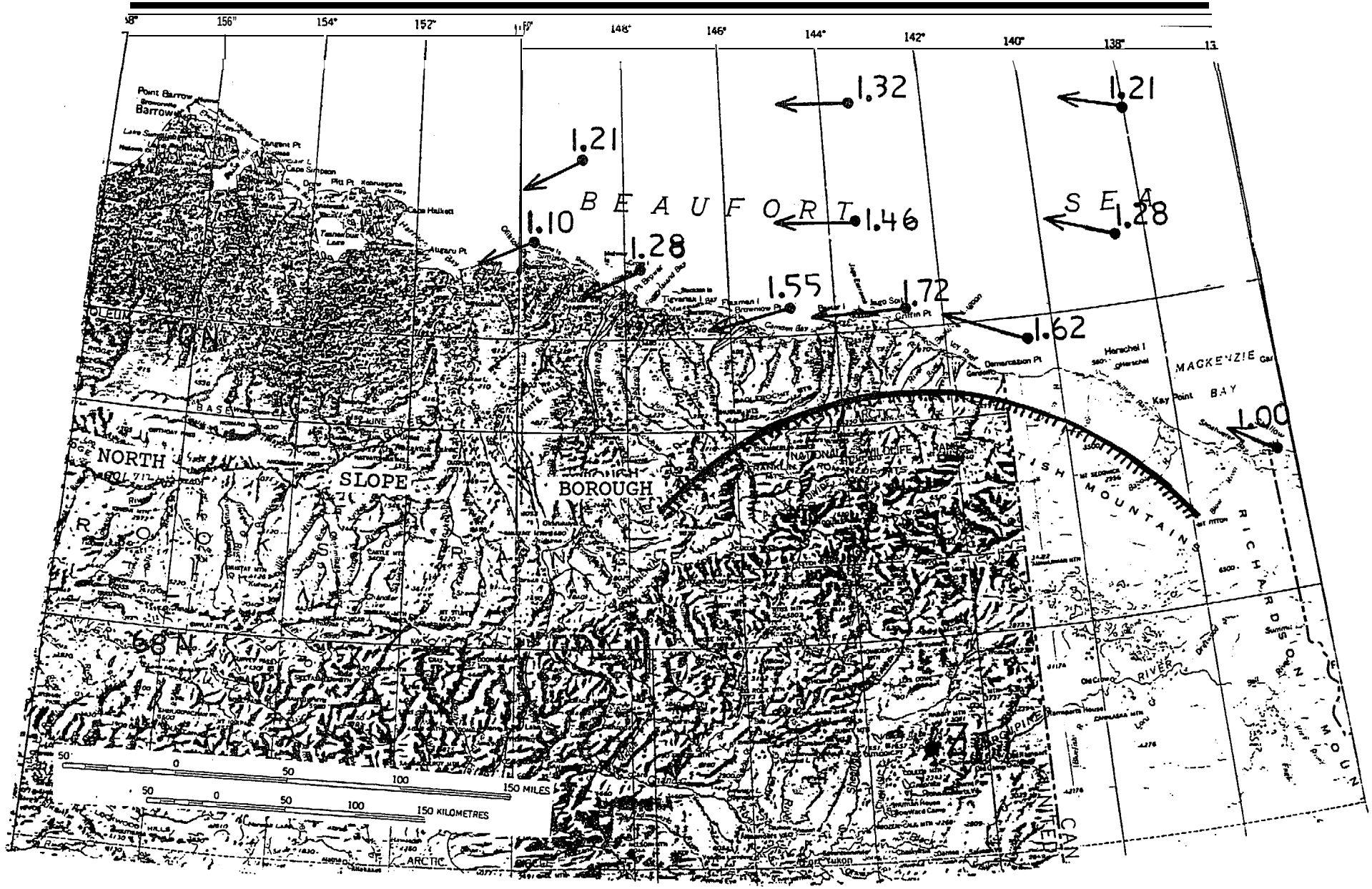


Figure 9. Model generated U velocities in multiples of $V_{\infty}$ magnitudes for $V_G$'s from the east.

less than 180°+ (direction to Z), the site will be subject to clockwise (CW) flow around the mountain barrier or an eastward push.

Figure 5 shows the theoretical winds in multiples of a westerly $V_G$. The nearshore winds are supergeostrophic from Prudhoe Bay to Herschel Island and decrease in magnitude seaward. Figure 6 shows theoretical winds in multiples of a northwesterly $V_G$. The coastal winds from Harrison Bay to Camden Bay are subgeostrophic and increase in magnitude as distance from the Brooks Range increases. The nearshore winds from Barter Island to Mackenzie Bay are supergeostrophic and decrease in magnitude seaward. Figure 7 shows the wind pattern that evolves from a northerly wind. The nearshore winds from Harrison Bay to Herschel Island are now all subgeostrophic with velocities approaching geostrophic to the north. This is an example of "split" flow with winds west of Barter Island having an easterly heading and winds east of Barter Island having a westerly heading. The nearshore zone from Camden Bay to Demarcation Pt. will have drastically reduced winds. Figure 8 shows the wind pattern for an initial northeasterly wind. The coastal winds from Barter Island to Harrison Bay are supergeostrophic with little directional change but they diminish seaward. The nearshore winds from Barter Island to Herschel Island maintain their original speed but show directional changes which diminish seaward. The winds in the Mackenzie Bay area are greatly reduced. Figure 9 is the pattern caused by an initial easterly wind. The nearshore winds are supergeostrophic from Herschel Island west to Harrison Bay and their magnitudes diminish seaward.

Figure 2 shows the coastal coverage of pressure network CED. This coastal zone will undergo supergeostrophic winds for $V_G$'s from the east, northeast, west and northwest and will be subject to reduced winds for only northerly winds (see Figures 5-9) which are rare.

MODEL DESCRIPTION-BUOY TRAJECTORIES

Due to the unusual predominance of westerly winds along the Beaufort coast from August through October 1983, the average Coast Guard buoy motion was eastward. The $V_G$ data was calculated from three different pressure triangles (Fig. 2, chosen from six possible combinations). These triangles alternately contained the buoy trajectories (4518 and 4519) during most of their eastward drift. Triangles ABC, CED, and CDF were used in August, September, and October, respectively. Figure 10 shows the actual trajectories of buoys 4518 and 4519 (two longest lasting buoys) from August through October with the average monthly ice edges superimposed (NOAA/U.S. Navy Joint Ice Center, 1983). Buoy 4519 ran into shoals in August which caused it to stop movement for several days. It later "caught up" with buoy 4518 by 9 September and moved in a similar trajectory until 4518 ran into shallow water on 21 September ("died" 24 September). Buoy 4519 continued drifting in open water until 18 October when it was apparently frozen in or attached to pack ice. For comparison to the model derived buoy trajectories: buoy 4518 positions are used in August up to 6 September, the combined trajectories (Fig. 10) of 4519 and 4518 are used until 21 September, and the trajectory of buoy 4519 is used until 18 October.

As a preliminary model run, the initial buoy deployment position (4518) was used in conjunction with unmodified $V_G$'s generated by the appropriate pressure triangles (Fig. 2). This hypothetical buoy was advanced in the direction of $V_G$ + 180° (standard rhumbline navigational algorithm) at 3, 4, 5 and 6% of $V_G$. All of these trial runs without modification for flow around an obstacle resulted in the model buoy running into the shore after a month of drift. This inevitable fact and the actual individual buoy tracks

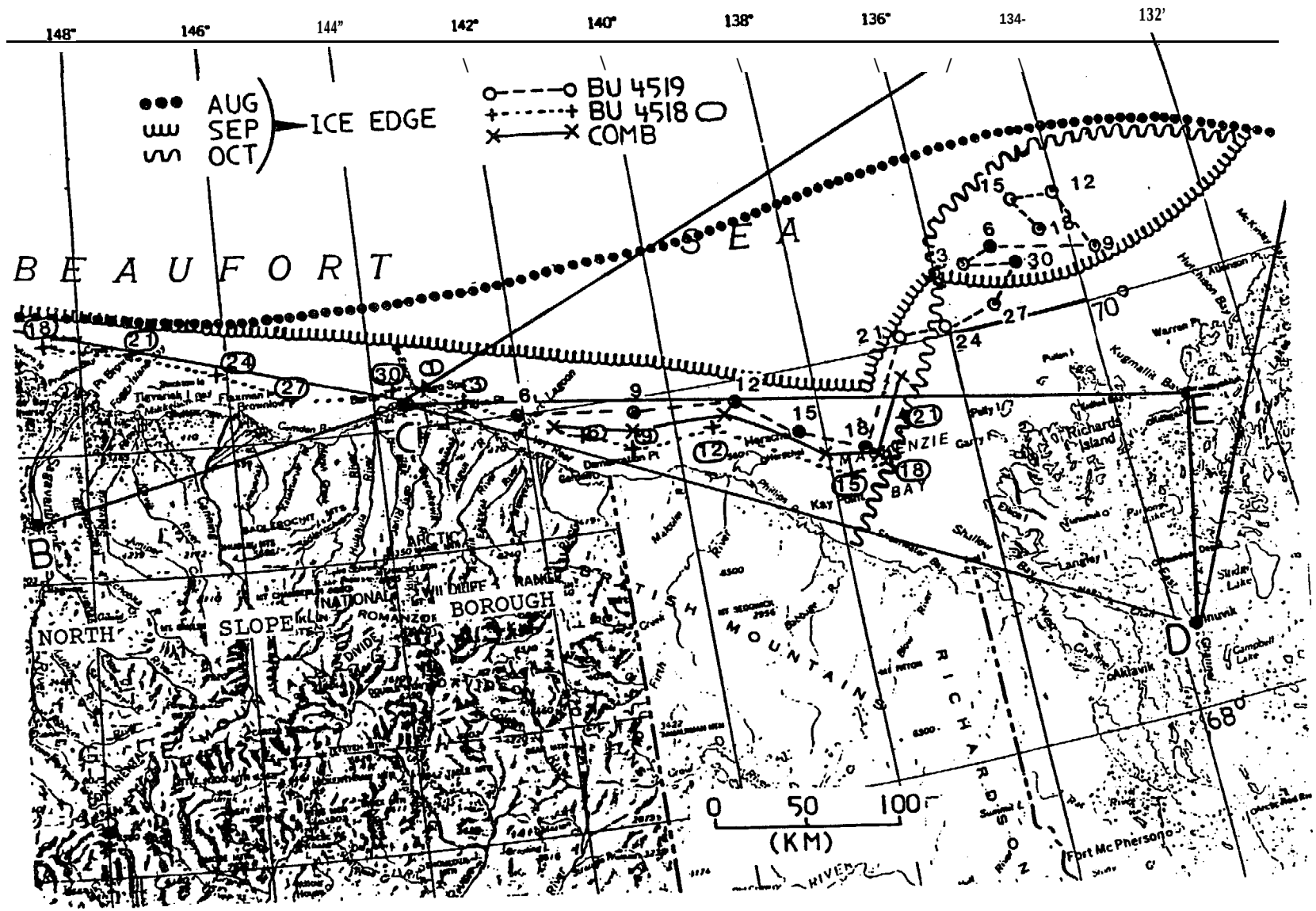


**Figure 10.** **Trajectories** of buoys 4518 and 4519 (U.S. Coast **Guard) during** **surrounding pressure triangles, and the average ice** **August, September and October 1983 are shown.** **unimpeded** drift. Parts of **edge (greater than 50% coverage) for** the combined trajectory for September is designated X. The buoys were deployed 18 August 1983. Starting west and moving eastward, days 18-30 represent August positions, days 1-30 represent September positions and days

indicating periods of increased and decreased drift speeds relative to each other for the same large scale wind, pointed to some position-dependent mesoscale headland effect operating along the eastern Alaskan Arctic coast.

The next set of model runs were those in which a hypothetical buoy was advanced with a $V_G$ ❑edified by orography, except when from 120° to 270° (see Model Description-Winds above). Therefore, modified flow U (see 3-5) or unmodified flow $V_G$ (if direction is from 120° to 270°) is used to advance a hypothetical buoy in the U or $V_G$ + 180° direction at 3, 4, 5 and 6% of their respective magnitudes.

A third set of runs used the same procedure as above, but geostrophic winds were smoothed in speed and direction before the orographic modification was applied. This was tried because large changes in speed and direction within the basic model interval of 3 hrs do not represent geostrophic balance conditions. In these cases, the effects of the rapidly changing wind field are not transmitted instantaneously to the actual buoys.

The best fit to the actual buoy trajectories (combined tracks of 4518 and 4519) can be seen in Figure 11. This was obtained by using the modified wind scheme without smoothing for August and September and the unmodified $V_G$ for October. The simple October fit was probably due to several causes: the real buoy was in a location that was probably not affected by orography; the real buoy was in deeper water (> 100 m) and not affected by bathymetry, and the model buoy was farther south and would have been (theoretically) affected by orography. The percentage of the modified or unmodified wind speeds used to advance the model buoy was 4% for trajectories (see Figs. 2 and 11) contained in triangle ABC (August), 2% for trajectories contained in triangle CED (September), and 4% for trajectories governed by CDF (October). Reynolds et al. (1985) recently found that ice floes in the southern Bering Sea

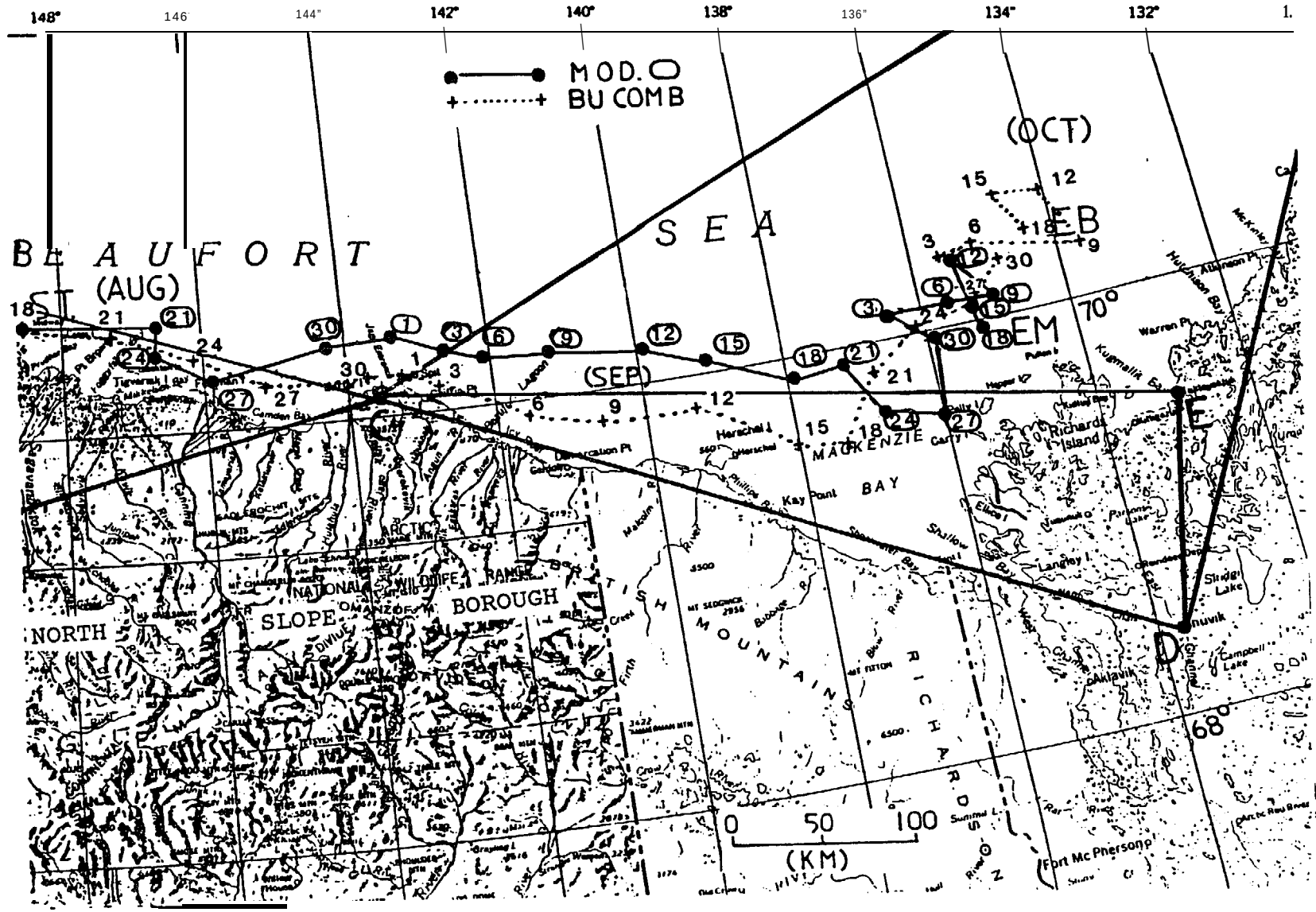


Figure 11. The combined 4518 and 4519 drift compared to the model drift. Again the pressure triangles are shown in part. The buoys were deployed 18 August 1983 (ST) and were locked into the sea ice by 18 October 1983 (EM ≡ last model buoy position; EB ≡ last actual buoy position).

marginal ice zone (MIZ) drifted at 4% of the surface wind speed (away from orographic effects). A main reason that only 2% of the speed was needed to drive the model buoy in September was that the triangle CED covers a coastal area subject to supergeostrophic enhancement of winds (see Figs. 5, 6, 8, 9). The major discrepancy between the purely wind driven model buoy motion and the actual buoy motion occurred during the 21-27 September period. Figure 12 shows the bathymetry in the Mackenzie Bay area and its effect on wind driven surface currents under a large scale wind from the northwest (MacNeill and Garrett, 1975). The model buoy drift from 21-27 September reflects a net wind from the northwest pushing the hypothetical buoy to the southeast. Figure 12 shows that the actual buoy was in shallow water between 10 m and 50 m. The piling up of water in this shallow area would produce a northeast to east contour-following water movement which did not allow the real buoy to move southeast. If the wind driven surface currents were in deeper water, out of the effects of the bottom, the actual buoy and model buoy would be less than 20 km apart after 60 days instead of 50 km apart. In either case, the technique appears to work quite well and explains 90% of the actual motion (on a distance basis). This success adds to the belief that the model describes the winds accurately in this area of the Beaufort Sea.

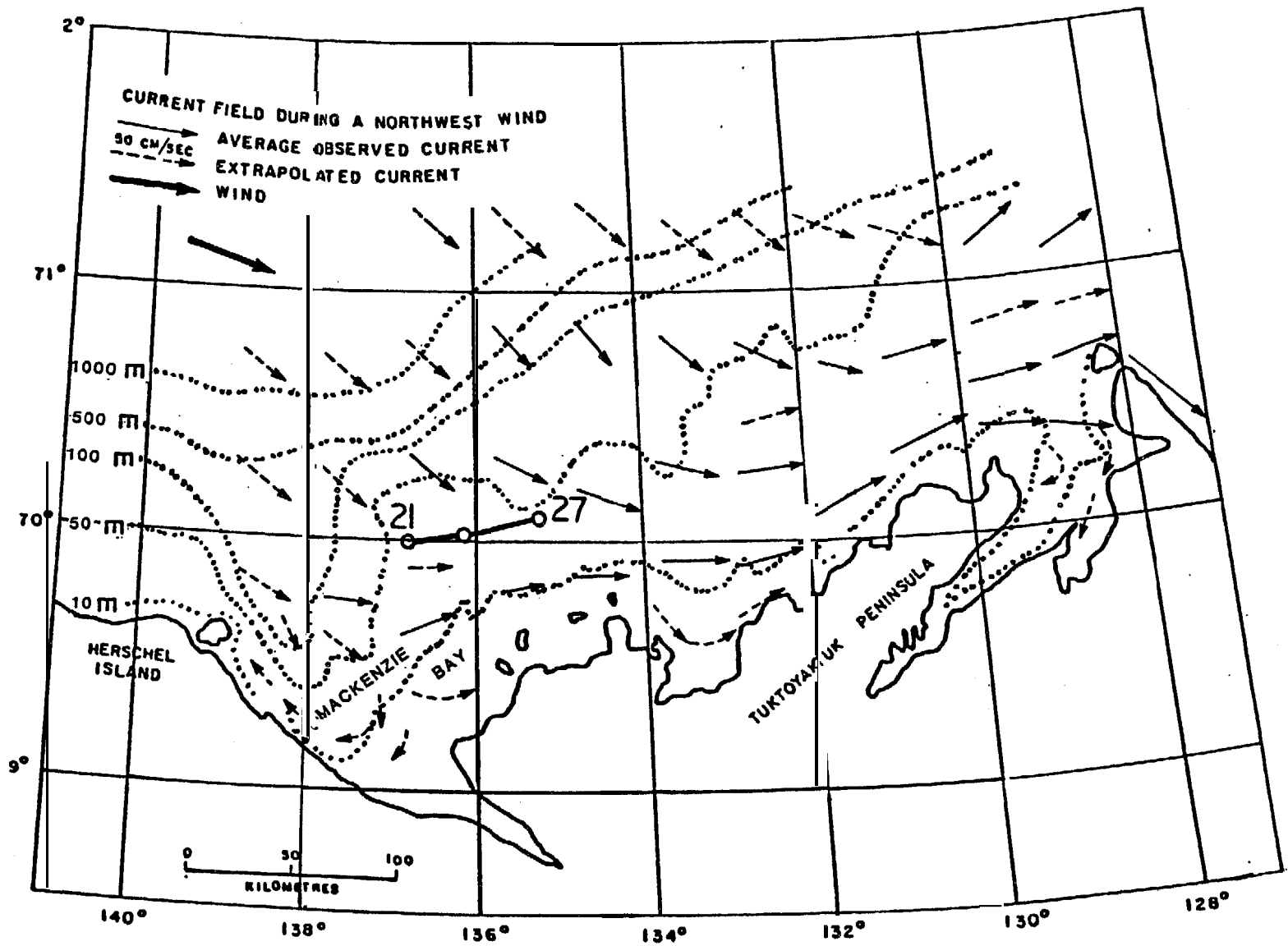


Figure 12. The bathymetry in the Mackenzie Bay area and its effect on wind driven surface currents (after MacNeill and Garrett, 1975). Actual buoy drift for 21-27 September 1983 shown as 0-0-0.

# SUMMARY AND CONCLUSIONS

The effect of a large headland on the wind field in a coastal zone has been modeled and carried one step beyond in an effort at "ground truthing". Actual buoy trajectories along a coastal zone which has predominant wind driven surface currents were compared with model generated buoy trajectories driven by headland modified winds. The model and buoy trajectories were very similar. After 60 days and 650 km of total drift, they were 50 km apart. The main discrepancy occurred when the actual buoy moved into a shallow part of the Mackenzie Bay. There the surface current in response to a northwesterly wind was constrained to flow to the northeast instead of the southeast.

The model uses high resolution mesoscale atmospheric pressure networks to define the pressure gradient wind $V_G$ offshore which becomes its initial input. These networks are land based and, therefore, do not require drifting satellite-transmitting pressure buoys with a low life expectancy (- 6 months) in arctic offshore environs. A simple extension of of Dickey's (1961) work to offshore areas and the open water season allows basic hydrodynamic considerations to be applied. The network $V_G$ is modified by flow around the 600 m contour of the Brooks Range. Areas of supergeostrophic and subgeostrophic flows are easily delineated in designated offshore areas.

In using the model, a number of parameters can be varied from which new insight may be gained. For example, the simple act of changing the percentages of the driving wind speed allows the user to check on the degree of coupling between the wind and ocean. This could be an indirect check on stability of the atmosphere. The time between onset of a wind velocity and

application of this wind to drive the buoy can also be changed. This allows for calculation of the lag time between onset of a pressure pattern and the actual flow realized. Figure 13 is a simple flow chart for the model.

## WIND-DRIVEN MODEL FLOW CHART

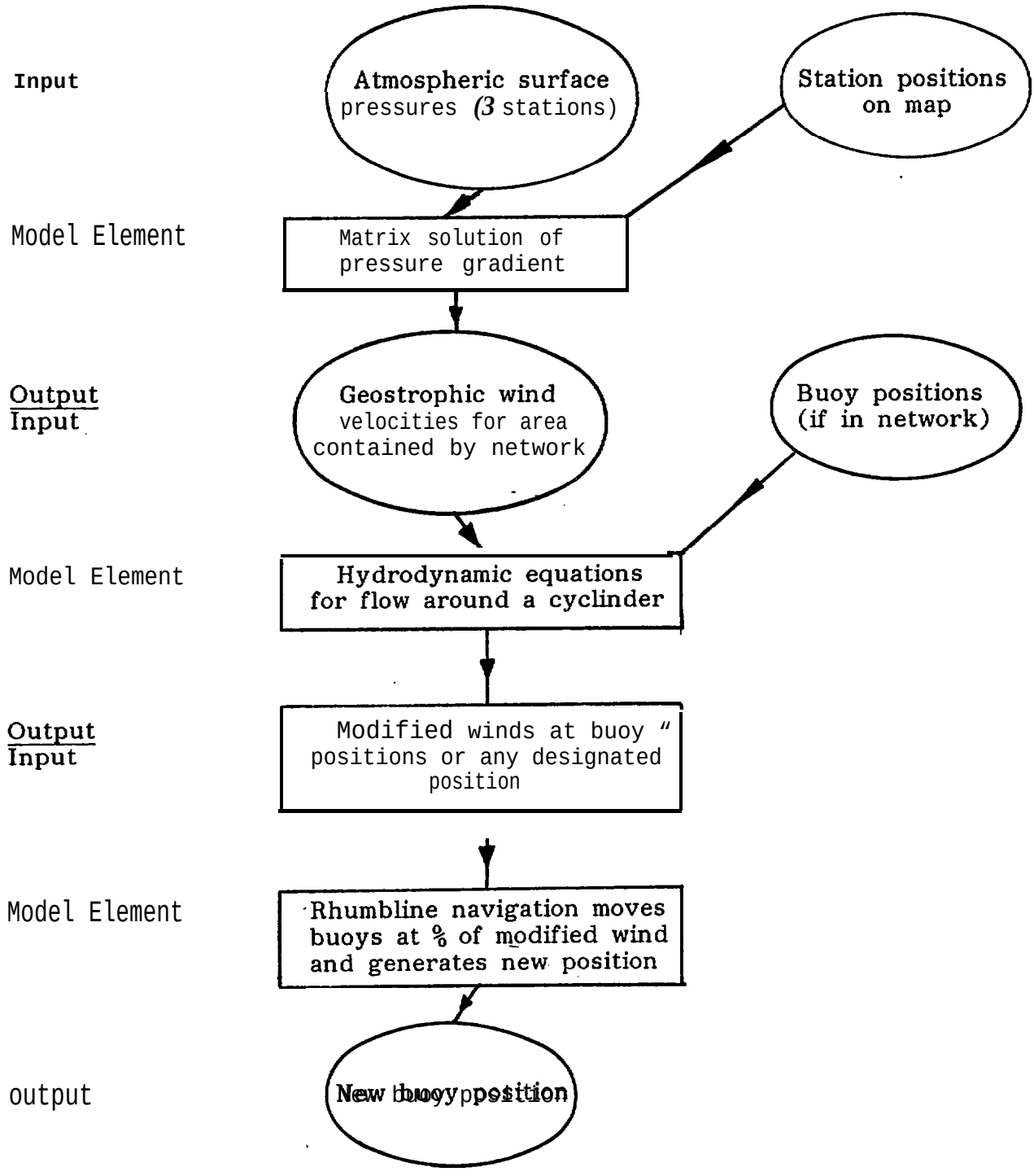


Figure 13. Flow chart for the wind-driven model.

## FUTURE WORK

The degree of coupling between the atmosphere and the ocean from July through October can be examined through use of buoy deployment within one fixed pressure network. The amount of buoy drift for a given network $V_G$ and atmospheric sounding can be compared. Atmospheric blockage by the Brooks Range can also be assessed. For a given large scale wind direction from 120° to 270°, coastal surface winds can be measured, mesoscale network winds can be derived and actual buoy movement at varying distances offshore recorded. A comparison of the large scale wind computed from NWS maps, mesoscale network winds, surface winds and actual buoy movement should provide many answers.

## ACKNOWLEDGMENTS

This Study was funded by the Minerals Management Service, U.S. Department of the Interior, through interagency agreement with the National Oceanic and Atmospheric Administration; U.S. Department of Commerce, as part of the Outer Continental Shelf Environmental Assessment Program. I wish to also thank R. Q. Robe of the U.S. Coast Guard R & D Center, Avery Point, Connecticut, for the use of his buoy data.

# REFERENCES


Aagaard, K. 1984. The Beaufort Undercurrent, *in The Alaska Beaufort Sea: Ecosystems and Environment.* Edited by P. Barnes, D. Schell and E. Reimnitz. Academic Press, New York, pp. 47-71

Albright, M. 1978. Construction of atmospheric surface pressure "maps from the AIDJEX data set. AIDJEX Bull., 39:111-120. University of Washington, Seattle

Albright, M. 1980. Geostrophic wind calculations for AIDJEX, *in A symposium on sea* ice *processes and models.* Edited by R. S. Pritchard. Proc. Intern. Comm. on Snow and Ice/Arctic Ice Dynamics Joint Experiment. University of Washington Press, Seattle, pp. 402-409

Batchelor, G. K. 1967. An Introduction to Fluid Dynamics. University Press, Cambridge, Mass. 615 pp.

Bessis, J. L. 1981. Operational data collection and platform location by satellite. Remote Sensing of Environment. 11:93-111.

**Brewer, W. A., Ii. D. Diaz, A. S. Prechtel, H. W. Searby and J. L. Wise. 1977**. *Climatic Atlas of the Outer Continental Shelf Waters and Coastal Regions* of *Alaska.* Vol. 111. AEIDC, University of Alaska, Anchorage and U.S. National Climatic Center, Asheville, NC., 409 pp".

Crossley, A. F. 1938. Note on the variation of pressure accompanying a distortion of air flow. Quart. J. Royal Meteorol. Sot., Vol. 64, p. 477.

Dickey, W. W. 1961. A study of a topographic effect on wind in the Arctic. J. Meteorol. 18:790-803.

Henry, R. F. 1975. Storm surges. Beaufort Sea Tech. Rpt. #19, Beaufort Sea Proj., Dept. of the Environment, 512 Federal Bldg., 1230 Government St., Victoria, B. C. V8W1Y4, 41 pp.

Kozo, T. L. 1980. Mountain barrier baroclinity effects on surface winds along the Alaskan Arctic Coast. Geophys. Res. Ltrs. 7:377-380.

Kozo, T. L. 1982. An observational study of sea breezes along the Alaskan Beaufort Sea coast. Part 1. J. Appl. Meteorol. 12:891-905.

Kozo, T. L. 1984a. Mesoscale wind phenomena along the Alaskan Beaufort Sea coast, *in The Alaskan Beaufort Sea: Ecosystems and Environments.* Edited by P. Barnes, D. Schell and E. Reimnitz. Academic Press, New York, pp. 23-45

Kozo, T. L. 1984b. Mountain barrier baroclinicity effects on surface winds along the Alaskan Arctic coast and offshore. Abstract in the 1984 Arctic Science Conf. (35th Alaskan Conf.), Oct. 2-5, 1984, Anchorage, sponsored by Amer. Ass. for Adv. of Sci-Arctic Div., Amer. Meteorol. Sot. and Arctic Inst. of North America, 109 pp.

Kozo, T. L. 1984c. Mesoscale meteorology, *in Environmental Characterization and Biological Use of Lagoons in the Eastern Beaufort Sea.* Edited by J. c. Truett. Final Reports of Principal Investigators, 24:129-579, NOAA-OMA-OAD, Alaska Office, 701 C St., P.O. Box 56, Anchorage, pp. 469-500.

MacNeill, M. R. and J. F. Garrett. 1975. Open water surface currents in the southern Beaufort Sea. Beaufort Sea Tech. Rpt. #17, Dept. of the Environment, 512 Federal Bldg., 1240 Government St., Victoria, B.C. V8W1Y4, 113 pp.

NOAA/U.S. Navy Joint Ice Center. 1983. Eastern-western Arctic sea ice analysis. Naval Polar Oceanogr. Ctr., Navy Dept., 4301 Suitland Rd., Washington, D.C. 20390

Reynolds, M., C. H. Pease and J. E. Overland. 1985. Ice drift and regional meteorology in the southern Bering Sea: Results from MIZEX West. J. Geophys. Res. 90:11,967-11,981.

Robe, R. Q., I. J. Lissauer, and T. L. Kozo. 1984. Beaufort Sea coastal" currents. 1983 Abstract in 1984 Arctic Science Conf. (35th Alaskan Conf.), Oct. 2-5, 1984, Anchorage, Alaska, sponsored by Amer. Ass. for Adv. of Sci-Arctic Div., Amer. Meteorol. SoC. and Arctic Inst. of North America. 109 pp.

Rogers, J. C. Meteorological factors affecting Inter-annual variability of summertime ice extent in the Beaufort Sea. Mon. Weather Rev., 106:890-897.

Schwerdtfeger, W. 1979. Meteorological aspects of the drift of ice from the Weddell Sea toward the mid-latitude westerlies. J. Geophys. Res. 84:6321-6328.